Frictional contact of two spheres for arbitrary 2D loading

Vladislav Aleshin, Koen van den Abeele

▶ **To cite this version:**

Vladislav Aleshin, Koen van den Abeele. Frictional contact of two spheres for arbitrary 2D loading. CFM 2011 - 20ème Congrès Français de Mécanique, Aug 2011, Besançon, France. 10.1121/1.3670734 . hal-03422634

HAL Id: hal-03422634
https://hal.science/hal-03422634

Submitted on 9 Nov 2021

HAL is a multi-disciplinary open access archive for the deposit and dissemination of scientific research documents, whether they are published or not. The documents may come from teaching and research institutions in France or abroad, or from public or private research centers.

L'archive ouverte pluridisciplinaire **HAL**, est destinée au dépôt et à la diffusion de documents scientifiques de niveau recherche, publiés ou non, émanant des établissements d'enseignement et de recherche français ou étrangers, des laboratoires publics ou privés.

Frictional contact of two spheres for arbitrary 2D loading

V. ALESHIN[a], K. VAN DEN ABEELE[b]

a. *Institut d'Electronique, de Microélectronique et de Nanotechnologie, (IEMN-DOAE UMR CNRS 8520), 59651 Villeneuve d'Ascq (France)*
b. K.U.Leuven Campus Kortrijk, E. Sabbelaan 53, 8500 Kortrijk (Belgium)

Résumé :

L'interaction avec friction entre deux sphères élastiques est un problème fondamental de la mécanique du contact. Le déplacement tangentiel dépend de la force normale et tangentielle de manière complexe et, habituellement, hystérétique. Nous analysons en détails la caractéristique clef de la mémoire du système (la distribution de la contrainte de cisaillement sur la zone de contact) et nous identifions les différents régimes qui apparaissent en fonction des conditions variables de chargement. La distribution complète de la contrainte de cisaillement dépend du régime actuel et, en plusieurs cas, d'un certain régime passé. Le schéma général de l'organisation de la mémoire est établi, ce qui permet de décrire de manière universelle le comportement mécanique du système et cela quelque soit l'historique du chargement. Les diagrammes de mémoire proposés ici permettent d'obtenir sous forme algorithmique une solution générale analytique du problème.

Abstract :

Frictional interaction of two elastic spheres is a fundamental problem of contact mechanics. The tangential displacement depends on the normal and tangential force in a complicated and, in general, hysteretic manner. We analyze in detail the key memory characteristic of the system (the traction distribution in the contact zone) and identify various regimes appearing under various loading conditions. The full traction distribution depends on the current regime and, in many cases, on some previous regime. A general scheme of memory organization is established that enables to describe in a universal way the system's behavior for all possible loading histories. The memory diagrams proposed here provide a computer-assisted general solution to the problem.

Mots clefs : Hertz-Mindlin, contact mechanisms, hysteresis, friction, stick-slip

1 Introduction: basic particular solutions

The history of the contact problem for two rough spheres (frequently called the Hertz-Mindlin or HM problem) dates back to 1880s when H. Hertz found the classical solution [1] for purely normal compression. As it was shown, the normal displacement a and the contact radius c are linked to the normal force N by relationships

$$a = \left(KR^{-1/2}N\right)^{2/3}, \quad c = \left(KRN\right)^{1/3} \tag{1}$$

respectively, in which R is the sphere's radius and $K=3(1-\nu^2)/(4E)$ where ν and E are the Poisson's ratio and the Young's modulus of the material. The distribution of the normal stress in the contact spot is given by

$$\sigma(\rho) = 3\left(2\pi KR\right)^{-1}\sqrt{c^2-\rho^2}\,, \tag{2}$$

with ρ, the polar coordinate. Thus, the values a, c, and the distribution $\sigma(\rho)$ always depend on the normal force N in a simple and nonhysteretic manner.

This is not so for the tangential displacement b and the shear stress (traction) $\tau(\rho)$ that are created if a tangential force T is added. Then, as it has been shown by Cattaneo [2] and Mindlin [3], even a small force $T>0$ will result in a creation of a slip annulus $s<\rho\le c$ that propagates inward (s decreases) as T increases. The

rest $\rho \le s$ of the contact zone remains stuck. The boundary s between stick and slip zones can be found [4] as

$$s = \left[KR\left(N - T/\mu \right) \right]^{1/3}, \tag{3}$$

and the traction distribution

$$\tau(\rho) = H_c^s(\rho) \equiv \frac{3\mu}{2\pi KR} \begin{cases} \sqrt{c^2-\rho^2} - \sqrt{s^2-\rho^2}, & \rho < s \\ \sqrt{c^2-\rho^2}, & s \le \rho \le c \\ 0, & c < \rho \end{cases}, \tag{4}$$

is given by the Cattaneo-Mindlin function $H_c^s(\rho)$ that guaranties the Coulomb friction law $\tau(\rho)=\mu\,\sigma(\rho)$ in the slip zone. The application of the tangential force results in the tangential displacement

$$b = \kappa \left(KR \right)^{-2/3} \left(c^2 - s^2 \right), \tag{5}$$

where κ is a combination of material constants, $\kappa=(2-\nu)\mu K^{2/3}/[2(1-\nu)\mathrm{R}^{1/3}]$. The original demonstration [3] addresses the case N=const.

The incremental procedure proposed in [4] that consists in assuming small variations ΔN and ΔT and application of the solution (3)-(5) makes it possible to prove [4,5] that this solution holds for changing N as well, in the case $\mu\, dN/dT<1$ ($T>0$). If $\mu\, dN/dT \ge 1$ the incremental procedure provides the following result: the slip zone is absent i.e. $s=c$, and

$$\tau(\rho) = R_{c(0)}^{c(T)}(\rho), \tag{6}$$

where

$$R_{c(T_1)}^{c(T_2)}(\rho) \equiv \int_{T_1}^{T_2} dT' \begin{cases} \dfrac{1}{2\pi c(T') \sqrt{c(T')^2 - \rho^2}}, & \rho \le c(T') \\ 0, & c(T') < \rho \end{cases}, \tag{7}$$

with the $c(T)$ resulting from $N(T)$ according to (2). Note that the existence of functional dependence $N=N(T)$ is an important applicability condition for the whole theory. The displacement b can be obtained by integration of

$$db/dT = 2\kappa (3\mu)^{-1} N^{-1/3}(T). \tag{8}$$

Equations (3)-(5) and (6)-(8) represent particular solutions (called here H-regime and R-regime, respectively) valid for a first loading curve, i.e. when the contact zone initially was free of traction. Another important requirement is that one of the conditions $\mu\, dN/dT<1$ for the H-regime or $\mu\, dN/dT \ge 1$ for the R-regime must be satisfied during all loading history. The main problem of the HM system is how to extend these solutions for the case when $\mu\, dN/dT$ can be lower and higher that 1 at different moments of time, and for the case when $\mathrm{sgn}(dT/dt)$ changes i.e. the first loading curve is completed. Here we call these events "regime transformations" and "switching".

2 Regime transformations

Here we consider several examples for regime transformations that enable to understand the general principle and then construct memory diagrams containing the complete information about the history of the system.

The simplest example is switching during the H-regime. Suppose that the initial loading of the system by a decreasing force T was followed by an increasing branch that started at minimum $T=T_1$. At that point 1, with the stick-slip boundary $s=s_1$ and the contact radius $c=c_1$, the traction distribution $\tau_1(\rho) = H_{c_1}^{s_1}(\rho)$ satisfied two conditions: for $\rho \le s_1$, points at the opposite contact faces do not slip, and, for $s_1 \le \rho \le c_1$, the traction is given by the Coulomb friction law $\tau_1(\rho)=-\mu\,\sigma_1(\rho)$. It is straightforward to show that, by addition of the

combination $H^s_{c_1}(\rho)+H^s_c(\rho)$ to the traction, two other conditions will be met: absence of slip for $\rho \le s$ and the Coulomb friction law $\tau(\rho)=\mu\,\sigma(\rho)$ in the slip annulus $s \le \rho \le c$. Therefore, the result for traction is

$$\tau(\rho)=\tau_1(\rho)+H^s_{c_1}(\rho)+H^s_c(\rho), \tag{9}$$

hence, by integration over the contact spot,

$$T=T_1+\mu\left(N_1-(KR)^{-1}s^3\right)+I\mu\left(N-(KR)^{-1}s^3\right), \tag{10}$$

from which s can be easily found, and

$$b=b_1+\kappa\left(N_1^{2/3}-(KR)^{-2/3}s^2\right)+\kappa\left(N^{2/3}-(KR)^{-2/3}s^2\right). \tag{11}$$

Suppose then that at point 2 at $T=T_2$ the combination $\mu\,dN/dT$ exceeds 1, so that the system enters into the reversible regime. In this case, the traction distribution is given by

$$\tau(\rho)=\tau_2(\rho)+R^{c(T)}_{c(T_2)}(\rho). \tag{12}$$

where $\tau_2(\rho)$ is obtained from (9) by assuming $T=T_2$. In the reversible regime, no special efforts are needed to guarantee the Coulomb relationship in the slip zone, since this zone is absent ($s=c$). The displacement

$$b=b_2+\frac{2\kappa}{3\mu}\int_{T_2}^{T}\frac{dT'}{N^{1/3}(T')}, \tag{13}$$

in accordance to (8).

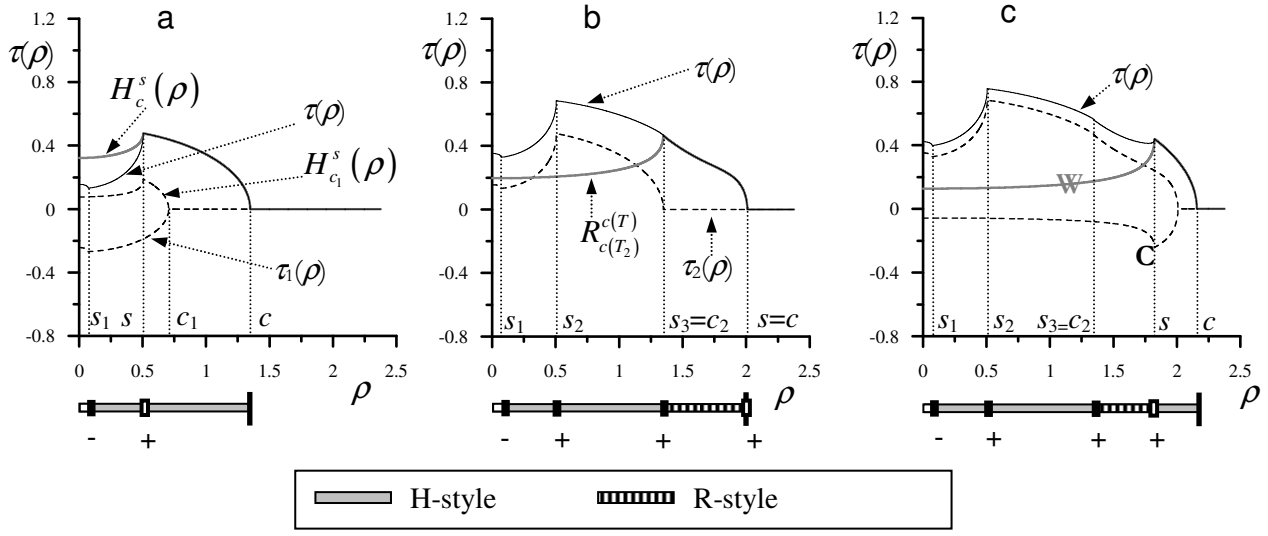

FIG. 1 – Traction distributions in the considered example and corresponding memory diagrams. (a) Traction distribution (10) with its components that illustrate stitching in the H-regime (H+H transformation); (b) traction distribution (13) in the zone with $\mu\,dN/dT>1$, i.e. after H+R transformation; (c) traction (15) after R+H transformation. Filling styles used in the diagrams are defined in the legend at the bottom of the plot.

Now suppose that at the point 3 ($T=T_3$) the combination $\mu\,dN/dT$ becomes again less than 1. Then slip has to develop anew, again from the contact boundary c, and, similarly to the first case considered, the Coulomb relationship has to be satisfied by addition of the compensation term in the form

$$\tau(\rho)=\tau_3(\rho)-R^{c(T_3)}_s(\rho)+H^s_c(\rho), \tag{14}$$

in which some part $R^{c(T_3)}_s(\rho)$ of the previously added traction $R^{c(T_3)}_{c(T_2)}(\rho)$ is removed. It can be shown that the new stick-slip boundary s is obtained via the system

$$\begin{cases} T = T_3 - T_C + \mu (KR)^{-1} \left(c^3(T) - s^3 \right) \\ c(T_3 - T_C) = s \end{cases}, \tag{15}$$

in which T_C is the tangential force corresponding to the compensation term $R_s^{c(T_3)}(\rho)$.

The details of this example can be found in [5]. The three regime transformations are illustrated in figure 1. Here for us the essential issue is that the full traction distributions can be coded is a way shown at the bottom of figure 1. In this compact representation, a sequence s_m (m=1...M) of the previously memorized stick-slip boundaries is plotted on the ρ-axis. A complete organization of memory in our problem would also include the information on a regime (H or R) responsible for the creation of each of points s_m and the signs I_m of the derivative dT/dt during these regimes. We call the proposed scheme a memory diagram; the principle of its creation and evolution is discussed below.

3 Memory diagrams

The memory diagram is a sequence of points $\{s_1, s_2, ..., s_M, s\}$ placed on the horizontal bar representing the ρ-axis between ρ=0 and ρ=c. The previously memorized stick-slip boundaries s_m (memory s-points) are marked with filled rectangles; they do not move with changing T. The last, hollow rectangle represents the movable s-point. The bar consists of sections colored with different color styles: white, H-style, and R-style (the latter two are chosen here as gray and hatched filling). At the first moment of time, the horizontal bar was colored in white; application of T resulted in appearance of the movable s-point shifting to the left that repaints the bar on its right in the H-style. At the moment 1, at which the sign of dT/dt changes, the moving s-point freezes and becomes a memory s-point (filled rectangle); a new movable point appears at ρ=c and starts shifting from the right to the left. This situation is shown in figure 1 (a) at the moment 2 when overloading (R-regime) is about to occur. At this time, two memory points are created: the first one s_2 is the former hollow point that becomes black and freezes, and the second one corresponds to the contact radius at the moment 2, s_3=c_2. Another, movable s-point coincides with contact radius (figure 1 (b)) that moves to the right. The section [s_3,s=c] created by the moving point s is colored in R-style. Leaving the R-regime and return to the H-regime make the points ρ=s and ρ=c to separate which is shown in figure. 1 (c); the movable point travels to the left and again repaints the bar in the H-style.

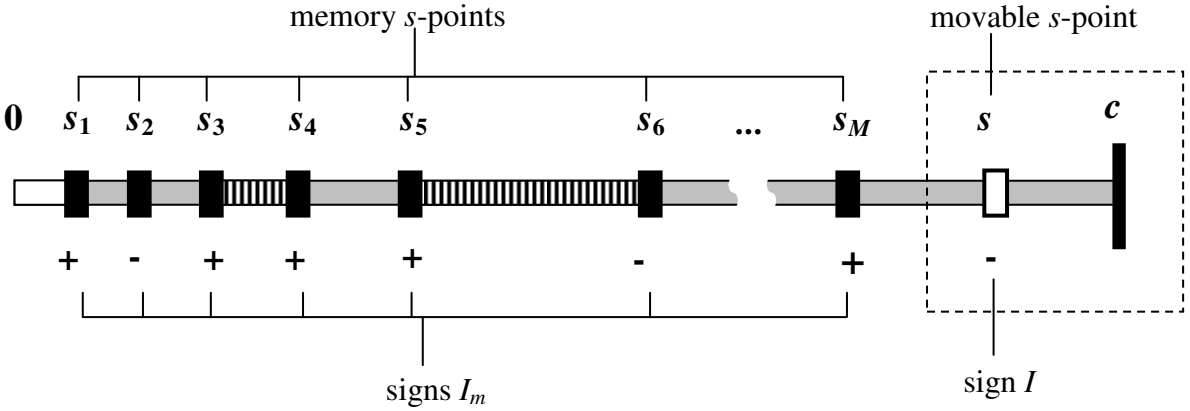

FIG. 2 – Memory diagram for the HM problem for an arbitrary loading protocol $T(t)$. The memorized stick-slip boundaries s_m (m=1..M) are placed on the ρ-axis and marked with filled rectangles, while the actual stick-slip boundary s (moving) in depicted with a hollow rectangle. Filling style of sections between points s_m and s_{m+1}corresponds to the regimes responsible for the creation of the point s_m. Signs I_m of dT/dt in these regimes and current I=sgn(dT/dt) are marked below.

The considered example, despite on its simplicity, illustrates all possible regime transformations: H+H, H+R, and R+H. As we have seen, the H+H transformation creates one memory point and an H-styled section of the bar, the H+R transformation creates two memory points and an R-styled section, and the R+H transition does not produce any new memory point but repaints the R-style in the H-style. In the H-regime, the movable s-point always goes to the left and is different from the contact radius c. In the R-regime, the movable s-point always coincides with c and can move both to the left and to the right. In the H-regime, the last section

$s<\rho<c$ is always in the H-style. In the R-regime, the last section $s_M<\rho<s=c$ is always in the R-style.

An application of a more complicated protocol $T(t)$ would result in a picture similar to those shown in figure 2. Such a portrait completely determines memory effects that can be encountered in the HM problem with 2D loading. Since the solution $b(T)$ to the problem at any moment of time depends only on the regime and the type of the compensation term, only the diagram ending (dashed window in figure 2) is essential for building up the curve $b(T)$. The rest of the memory diagram becomes important only if some memory points s_m, m=1...M, are erased. This happens if s suddenly becomes less than s_M. The process of erasing points is considered in detail is [5]. If one or more memory points are erased, M decreases, and new memory points with lesser m fall into the zone called "the diagram ending" and plotted in figure 2. All possible diagram endings are shown in figure 3.

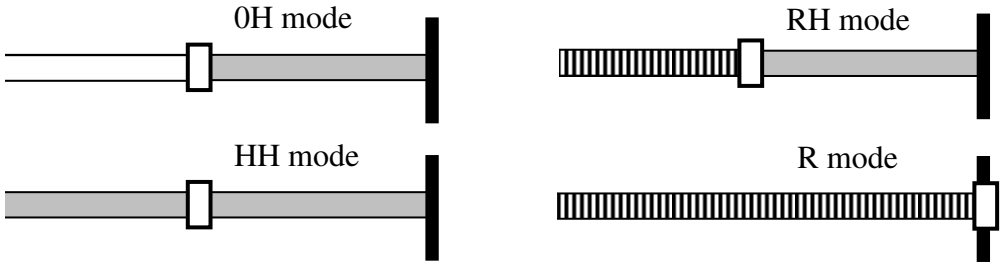

FIG. 3 – Memory diagram endings corresponding to modes 0H, HH, RH, and R.

4 Analytical solutions for different modes

Using the expressions (9)-(15) from the considered example, is it possible to derive the analogous solutions for various modes depicted in figure 3. So, for a given memory diagram with the ending of the type 0H, the resulting expressions for traction, stick-slip boundary and the tangential displacement are

$$\tau(\rho) = IH_c^s(\rho), \tag{16}$$

$$s = \left[KR\left(N - IT/\mu\right)\right]^{1/3}, \tag{17}$$

$$b = \kappa I\left[N^{2/3} - \left(KR\right)^{-2/3} s^2\right]. \tag{18}$$

The same characteristics in the HH mode are

$$\tau(\rho) = \tau_M(\rho) + I\left(H_{c_M}^s(\rho) + H_c^s(\rho)\right), \tag{19}$$

$$s = \left[KR\left(\frac{I}{2\mu}\left(T_M - T\right) + \frac{1}{2}\left(N_M + N\right)\right)\right]^{1/3}, \tag{20}$$

$$b = b_M + \kappa I\left(N^{2/3} + N_M^{2/3} - 2\left(KR\right)^{-2/3} s^2\right); \tag{21}$$

and for the R mode:

$$\tau(\rho) = \tau_M(\rho) + R_{c_M}^{c(T)}(\rho), \tag{22}$$

$$b = b_M + \frac{2\kappa}{3\mu}\int_{T_M}^{T} \frac{dT'}{N^{1/3}(T')}, \tag{23}$$

while the stick slip boundary $s=c$. Finally, in the RH mode,

$$\tau(\rho) = \tau_M(\rho) + R_{c_M}^s(\rho) + IH_c^s(\rho), \tag{24}$$

$$\begin{cases} T = T^* + I\mu\left(KR\right)^{-1}\left(c^3(T) - s^3\right) \\ c\left(T^*\right) = s \end{cases}. \tag{25}$$

In the last expression, T^* corresponds to the terms $\tau_M(\rho)+R^s_{c_M}(\rho)$ of (24) integrated over the contact spot. The displacement

$$b = b_M + \frac{2\kappa}{3\mu}\int_{T_M}^{T^*}\frac{dT'}{N^{1/3}(T')} + \kappa I\left[N^{2/3} - (KR)^{-2/3}s^2\right]. \tag{26}$$

The developed method, supplemented by the complete algorithm [5] for building up memory diagrams, enables to obtain in an automated way the solution $b(T)$ for any protocol $T(t)$ and loading condition $N(T)$. An example is given below (figure 4) for the situation when the protocol $T(t)$ creates two internal hysteretic loops, and the loading condition $N(T)$ is such that $\mu\, dN/dT>1$ in certain range of T.

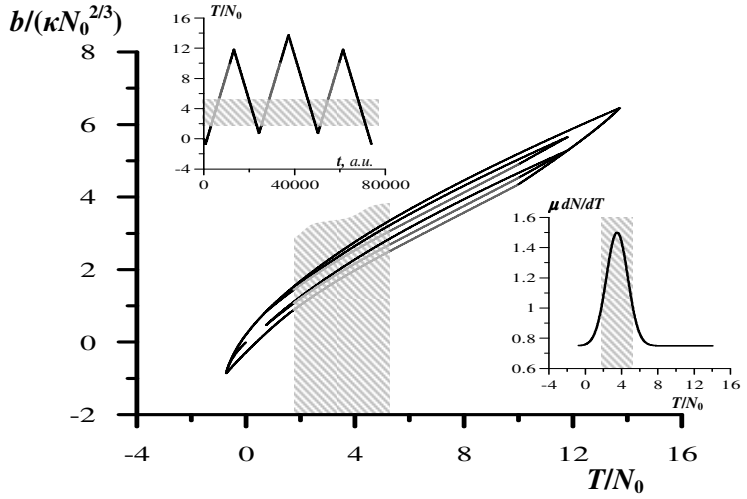

FIG. 4 – Hysteretic curve $b(T)$ for the protocol $T(t)$ (upper inset) that traces two internal congruent loops confined between the same extremum values. The loading condition (lower inset) is chosen such that in the whole T-range one overloading interval $\mu\, dN/dT>1$ takes place for increasing T (gray hatched band).

In the future, we intend to apply a general formalism describing hysteretic dependencies (Preisach space) to the HM problem similarly to as it was done in [6], in order replace the single-purpose memory diagrams description by a standard well-known procedure.

We address these results to a wide range of mechanical scientists or engineers dealing with contact mechanics, micro-scale contacts, vibrations of rough contacting surfaces with friction, granular materials, nonlinear acoustics including NDT applications, etc.

5 Acknowledgements

The authors gratefully acknowledge the support of the ANR (ANL-MEMS 2010 BLAN 923 01).

References

[1] Landau, L. D., Lifshits, E. M., 1993. Theory of Elasticity. Pergamon Press, Oxford.
[2] Cattaneo, C., 1938. Sul contatto di due corpi elastici: distribuzione locale degli sforzi. Accad. Lincei Rend. 27(6), 342–348.
[3] Mindlin, R. D., 1949. Compliance of elastic bodies in contact. J. Appl. Mech. 16, 259–268.
[4] Mindlin, R.D., Deresiewicz, H., 1953. Elastic spheres in contact under varying oblique forces. J. Appl. Mech., Trans. ASME 20, 327-344.
[5] Aleshin, V., Van Den Abeele, K. (submitted). Hertz-Mindlin problem for an arbitrary oblique 2D loading. Part I: General solution by memory diagrams. J. Mech. phys. Sol.
[6] Aleshin, V., Van Den Abeele, K., 2009. Preisach analysis of the Hertz-Mindlin system. J. Mech. Phys. Solids 57, 657-672.